Supplementary information

A photoluminescent folic acid-derived carbon dots functionalized magnetic dendrimer as a pH-responsive carrier for targeted doxorubicin delivery

Soheyla Karimi[a], Hassan Namazi[a,b,*]

[a]*Research Laboratory of Dendrimers and Nanopolymers, Faculty of Chemistry, University of Tabriz, P.O. Box 51666, Tabriz, Iran*

[b]*Research Center for Pharmaceutical Nanotechnology (RCPN), Tabriz University of Medical Science, Tabriz, Iran; E-mail address: namazi@tabrizu.ac.ir (H. Namazi).*

Experimental Methods

Materials

The Ferrous chloride tetrahydrate ($FeCl_2$. $4H_2O$), Methanol, Ferric chloride hexahydrate ($FeCl_3$. $6H_2O$), Ethanol, Ammonia (NH_3, 25%), Malic acid, 4-dimethylaminopyridine (DMAP), Tetraethyl orthosilicate (TEOS), 2,4,6-Triamino-1,3,5-triazine (or Melamine), Dry toluene, Sodium hydroxide (NaOH), Monopotassium phosphate (KH_2PO_4), Dimethyl sulfoxide (DMSO), Disodium hydrogen phosphate (Na_2HPO_4), Folic acid (FA), Sodium chloride (NaCl), Sodium acetate, Potassium chloride (KCl), and Acetic acid were acquired from Merck and used without further purification. 3-(4,5-dimethylthiazole-2-yl)-2,5-diphenyltetrazoliumbromide (MTT), N,N-dicyclohexylcarbodiimide (DCC), and 4′,6-diamidino-2-phenylindoledihydrochloride (DAPI) were obtained from Sigma-Aldrich. Fetal bovine serum (FBS), Roswell Park Memorial Institute 1640 growth medium (RPMI), Dulbecco's modified eagle medium (DMEM), and Penicillin streptomycin (PS) were provided from Gibco BRL Life Technologies. The Doxorubicin anticancer drug (DOX) was bought from Sobhan Pharmaceuticals Co. (Iran). All required solutions were prepared with distilled water.

FT-IR analysis

FT-IR spectrum of Fe_3O_4, Fe_3O_4@SiO_2, Fe_3O_4@SiO_2-G1, and Fe_3O_4@SiO_2-G2 is shown in Figure 1S.

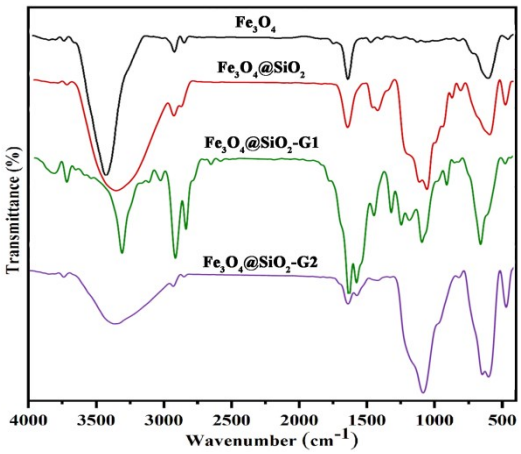

Figure 1S. FT-IR spectra of Fe_3O_4, Fe_3O_4@SiO_2, Fe_3O_4@SiO_2-G1, and Fe_3O_4@SiO_2-G2.

XRD analysis

To confirm the crystalline properties from synthesized dendrimer, X-ray diffraction (XRD) were studied. The X-ray diffraction (XRD) patterns of the prepared Fe_3O_4, Fe_3O_4@SiO_2-G2.5, and Fe_3O_4@SiO_2-G2.5-CDs are shown in Figure 2S. As seen in Figure 2S, the XRD patterns for Fe_3O_4@SiO_2-G2.5 exhibits a similar pattern with respect to Fe_3O_4. The Fe_3O_4@SiO_2-G2.5 display all diffraction peaks of pure Fe_3O_4 with a cubic spinel structure at 2Θ= 30.4°(220), 35. 9°(311), 43.4°(400), 54.1°(422), 57.5°(511), 63.06°(440), and 74.5°(533), indicating that Fe_3O_4 nanoparticles have been successfully connected with dendrimer. These characteristic diffraction peaks also indicating that the SiO_2 layer and Fe_3O_4@SiO_2-G2.5 did not lead to the crystalline phase change of Fe_3O_4 nanoparticles. Besides, a broad peak around 2θ= 10-25° appeared when the Fe_3O_4 nanoparticles were coated with silica and dendrimer layer, indicating the presence of amorphous silica shell and dendrimer layer [1] . However, the intensity of the diffraction peaks in the obtained pattern decreased with silica shells and then dendrimer molecules [2]. As all peaks were broadened because of Fe_3O_4 nucleus was covered step by step. Meanwhile, in the case of Fe_3O_4@SiO_2-G2.5, all broad peaks were shifted to lower angles because of the synergetic effect

of the amorphous SiO_2 and the Fe_3O_4@SiO_2-G2.5. The XRD patterns of Fe_3O_4@SiO_2-G2.5-CDs in Fig. 1c exhibited one diffraction peak at 2θ=22.6°, which was in good accordance with the disordered carbon atoms and the (002) graphite lattice [3]. These results confirm the successful synthesis of Fe_3O_4@SiO_2-G2.5-CDs.

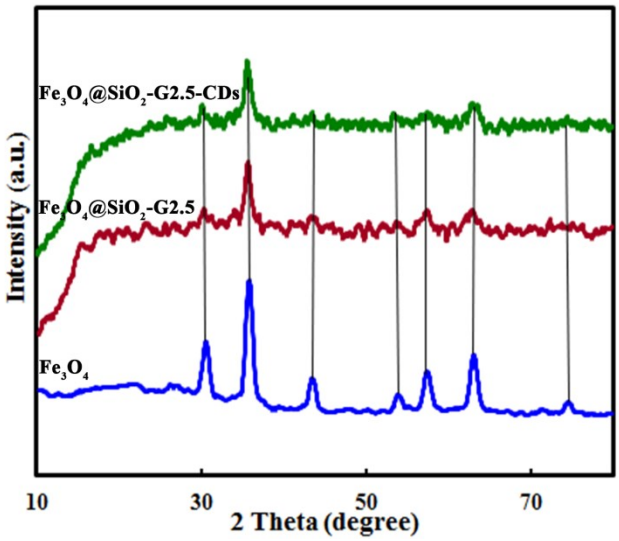

Figure 2S. XRD pattern of Fe_3O_4, Fe_3O_4@SiO_2-G2.5, and Fe_3O_4@SiO_2-G2.5-CDs.

UV-Vis and Fluorescence analysis

To further characterize the formation of Fe_3O_4@SiO_2-G2.5-CDs, UV-Vis absorption, fluorescence, and photoluminescence (PL) spectra of Fe_3O_4@SiO_2-G2.5, CDs and Fe_3O_4@SiO_2-G2.5-CDs were recorded (Figure 3S). As shown in Figure 3S, Fe_3O_4@SiO_2-G2.5 shows two maximum absorption bands at about 231 and 383 nm, which related to the n-π* electronic transitions of the aromatic C=N bonds and n-π* transitions of the C=O bonds, respectively. The UV-Vis absorption of CDs showed peaks at 233 nm and 320 nm, which can be related to the π→π* (C=C) and n→π* (C=O) transitions [3]. After grafting the CDs to the dendrimer surface, the UV-Vis spectra of the Fe_3O_4@SiO_2-G2.5-CDs exhibits two-band at 230, 320, and 432 nm that is

allocated to the presence of CDs and dendrimer on the surface of nanoparticles, respectively. As can be seen, the absorption intensity of Fe_3O_4@SiO_2-G2.5-CDs increased regard Fe_3O_4@SiO_2-G2.5 indicating grafted CDs onto the surface from dendrimer. This observation could confirm the successful formation of the Fe_3O_4@SiO_2-G2.5-CDs.

In this study, the fluorescence and photoluminescence properties of synthesized dendrimer were investigated and presented in Figure 3S. Under excitation by 320 nm a UV lamp, prepared CDs show blue photoluminescence with a strong emission peak at 400 nm [3]. The Fe_3O_4@SiO_2-G2.5--CDs show bright blue fluorescence color with emission bands at 396 nm as seen in Figure 3S. Therefore, obtained results suggested that these Fe_3O_4@SiO_2-G2.5-CDs may be used as a fluorescent probe.

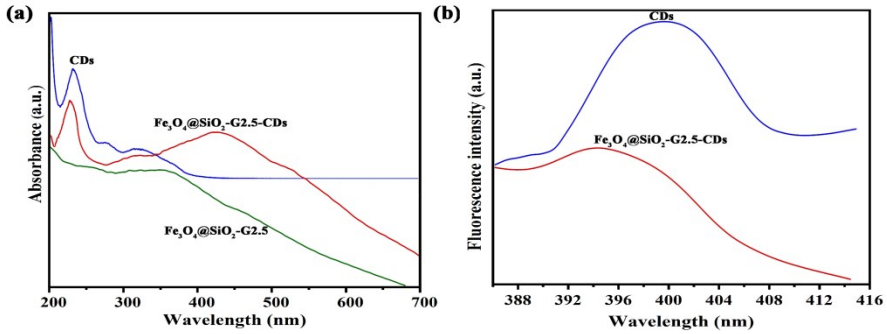

Figure 3S. (a) UV-visible absorption spectra of Fe_3O_4@SiO_2-G2.5, CDs, and Fe_3O_4@SiO_2-G2.5-CDs. (b) PL spectra of CDs and Fe_3O_4@SiO_2-G2.5-CDs in deionized water after excitation at 320 nm.

BET analysis

To further study the surface morphology and pore volume of the synthesized dendrimer, the N_2 adsorption-desorption isotherms experiments were performed. Figure 4S indicates the Barrett-Joyner-Halenda (BJH) plot and the nitrogen adsorption-desorption isotherm of the Fe_3O_4 and

Fe_3O_4@SiO_2-G2.5-CDs, respectively. It can be seen from Figure 3S that Fe_3O_4@SiO_2-G2.5-CDs exhibit a type IV plot with hysteresis loops of type H1 according to the IUPAC classification which is often related to a typical of mesoporous materials. The surface area, total pore volume, and mean pore diameter of the Fe_3O_4 and Fe_3O_4@SiO_2-G2.5-CDs were found to be 84.5 m^2/g, 0.4 cm^3/g, 15 nm, 66.4 m^2/g, 0.23 cm^3/g, 13.8 nm, respectively. According to resulted data, after Fe_3O_4 modified with dendrimer, the BET surface area, the total pore volume, and pore size decreased in comparison to Fe_3O_4 [4]. The decrease BET surface area indicates that COOH-malic acids were anchored onto the inner pore volume of Fe_3O_4@SiO_2 and grafting of carboxylic groups onto the pore surface produces contraction of the mesopore. This can be confirmed by the decrease in the pore volume of nanoparticles [5]. These results can confirm the formation of Fe_3O_4@SiO_2-G2.5-CDs. The high specific surface area of the Fe_3O_4@SiO_2-G2.5-CDs as a drug delivery system is a major advantage for adsorbing and storing drug molecules.

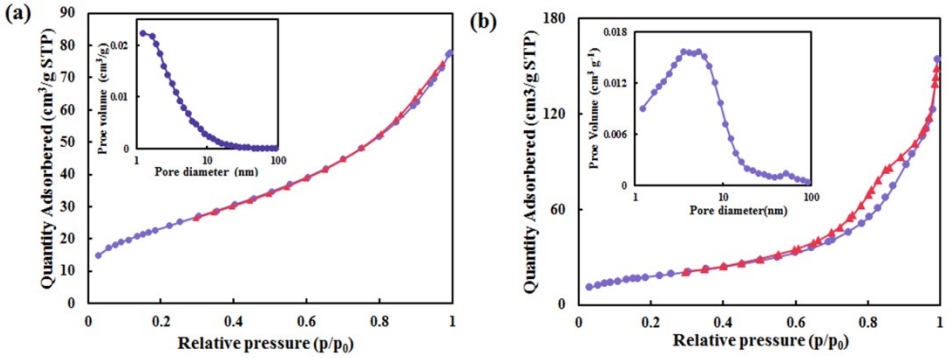

Figure 4S. Nitrogen adsorption-desorption isotherms and Barrett-Joyner-Halenda (BJH) plot of a) Fe_3O_4 and b) Fe_3O_4@SiO_2-G2.5-CDs carrier.

EDX analysis

The components of the Fe_3O_4@SiO_2-G2.5-CDs were also confirmed by energy-dispersive X-ray (EDX) spectrometry for Fe, Si, C, N, and O, as seen in Figure 5S. The presence of Fe, Si, O, C,

and N in Fe_3O_4@SiO_2-G2.5-CDs confirmed the correct synthesize of the dendrimer. The above results can be considered as direct evidence that Fe_3O_4@SiO_2-G2.5-CDs were successfully synthesized.

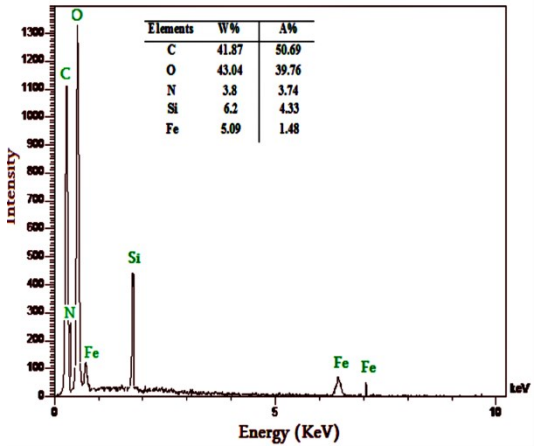

Figure 5S. EDX spectra of Fe_3O_4@SiO_2-G2.5-CDs.

VSM analysis

The magnetization measurements of the pure Fe_3O_4, Fe_3O_4@SiO_2, and Fe_3O_4@SiO_2-G2.5-CDs determined by VSM at 298 K (Figure 6S). The resulting magnetization curves revealed that the saturation magnetization value of pure Fe_3O_4, Fe_3O_4@SiO_2, and Fe_3O_4@SiO_2-G2.5-CDs were 67, 59, and 31.46 emu/g, respectively. The significant decline in the saturation magnetization values indicates an increase in the thickness of the coating layer on the surface of the magnetic core during the modification method. Consequently, the successful grafting of the Fe_3O_4@SiO_2-G2.5 on the Fe_3O_4 surface caused by the decrease of its magnetic responses. Nevertheless, the Fe_3O_4@SiO_2-G2.5-CDs can easily separate by an external magnetic field in less than 30 seconds, and also can re-dispersed immediately in solution under ultrasonication. In addition, the magnetization curves show zero remanences and coercivity, indicating the remarkable

superparamagnetic behavior of Fe_3O_4@SiO_2-G2.5-CDs [6]. Thus, the Fe_3O_4@SiO_2-G2.5-CDs are able to respond to an applied magnetic field for drug delivery systems.

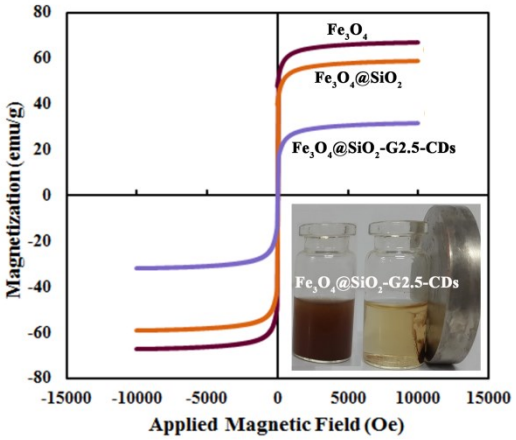

Figure 6S. VSM magnetization curves of the Fe_3O_4, Fe_3O_4@SiO_2, and Fe_3O_4@SiO_2-G2.5-CDs.

References

1. A. Zarei and S. Saedi, *J Inorg Organomet Polym Mater.,* 2018, **28**, 2835-2843.
2. Z. Fathi, E. Doustkhah, S. Rostamnia, F. Darvishi, A. Ghodsi and Y. Ide, *Int. **J**. Biol. Macromol.,* 2018, **117**, 218-224.
3. H. Liu, Z. Li, Y. Sun, X. Geng, Y. Hu, H. Meng, J. Ge and L. Qu, *Sci. Rep.*, 2018, **8**, 1-8.
4. K.-J. Kim and J.-W. Park, *J. Mater. Sci.,* 2017, **52**, 843-857.
5. M. Esmaeilpour, J. Javidi and F. Dehghani, *J. Iran. Chem. Soc.,* 2016, **13**, 695-714.
6. A. Landarani-Isfahani, M. Moghadam, S. Mohammadi, M. Royvaran, N. Moshtael-Arani, S. Rezaei, S. Tangestaninejad, V. Mirkhani and I. Mohammadpoor-Baltork, *Langmuir*, 2017, **33**, 8503-8515.